Gradient-Selected Zero-Quantum Experiments for the Study of $^1H—^{13}C$ Correlations in Protonated Methyl Groups

Michelle L. Gill and **Arthur G. Palmer, III**
Department of Biochemistry and Molecular Biophysics
Columbia University
New York, NY 10032

COLUMBIA UNIVERSITY MEDICAL CENTER

Abstract

Increased sensitivity of the HMQC pulse sequence, relative to its HSQC counterpart, for the study of $^1H—^{13}C$ correlations in fully protonated methyl groups, termed the methyl-TROSY effect, has been demonstrated [1-3]. Additional line narrowing is obtained by selective recording of the heteronuclear zero-quantum coherence (HZQC), rather than mixing the zero- and double-quantum signals, as in the HMQC experiment [4, 5].

The original $^1H—^{13}C$ HZQC pulse sequence [4, 5] is not well-suited for the study of smaller proteins or large proteins with flexible regions, because substantial differential relaxation during the t_1 evolution period is necessary to eliminate the outer multiplet components (HαHα and HβHβ) of the $^{13}C—^1H$ multiple-quantum signal. To address this issue, an HZQC pulse sequence has been developed in which the signals from the respective HαHα and HβHβ multiplet components are inverted in alternate acquisitions. Addition of the separate data sets results in cancellation of the undesirable signal components, while preserving the desired inner (HαHβ) multiplet component. The delays necessary for multiplet filtration conveniently allow incorporation of gradient coherence selection to eliminate the heteronuclear double-quantum signal without further lengthening the pulse sequence or extending the phase cycle. Two variations of the gradient selected HZQC, suitable for measuring multiple-quantum transverse relaxation rates (R_{ZQ} and R_{DQ}), are also presented. The sequences are validated using U-[^2H, ^{15}N], Ile δ1-[^{13}C $^1H_3$], Leu δ-[^{13}C $^1H_3$], Val γ-[^{13}C $^1H_3$] ribonuclease H from *E. coli*.

Methods

Sample Preparation

E. coli strain BL21(DE3) was transformed with a plasmid containing *E. coli* ribonuclease HI (RNase H) under control of a T7*lac* promoter. The cells were grown in 1 L of M9 minimal media containing 99.9% ^2H_2O, ^{15}N-ammonium chloride, and 98% $^2H_7$-glucose to OD_{600} = 0.7. Selective [^{13}C $^1H_3$]-labeling of Ile-δ1 and stereospecific labeling of Val/Leu-γ were achieved by supplementing the growth media with 80 mg/L of 2-keto-3-methyl-$^2H_3$-3-^2H-4-^{13}C butyric acid (99% ^{13}C, 98% ^2H, Cambridge Isotopes) and 50 mg/L of 2-keto-3-$^2H_2$-4-^{13}C-butyric acid (99% ^{13}C, 98% ^2H, Sigma Aldrich) an hour before induction [6, 7]. Purified U-[^2H, ^{15}N], Ile δ1-[^{13}C $^1H_3$], Leu δ-[^{13}C $^1H_3$], Val γ-[^{13}C $^1H_3$] RNase H NMR samples were 250 μM protein in 100 mM $^2H_3$-sodium acetate, pH 5.5 in 99% ^2H_2O.

NMR Spectroscopy

Spectra were acquired at 14.1, 18.8, and 21.1 T on Bruker DRX600 (14.1 T) and Avance spectrometers (18.8 and 21.2 T). Each spectrometer was equipped with a triple resonance z-axis gradient cryoprobe. Sample temperature was calibrated to 283 K using 98% $^2H_4$-methanol. Experiments collected at 14.1 T contained 8 scans per t_1 increment and 4096 × 640 points for $t_2 \times t_1$. At higher field strengths, 4 scans and 4096 × 1536 points were used. Spectral widths were 7.2 kHz × 3.8 kHz, 9.8 kHz × 4.4 kHz, or 10.8 kHz × 5.6 kHz ($t_2 \times t_1$) for 14.1, 18.8, and 21.1 T, respectively. Multipart experiments were acquired with identical t_1 points interleaved. HMQC [8, 9] and HZQC [4, 5] experiments were implemented as described. The HMQC experiment utilized the States-TPPI [10, 11] method for frequency discrimination, while all other experiments used the sensitivity-enhanced protocol [12].

Data Processing

Spectra were processed using NMRPipe [13]. To preserve lineshape features, data used for analysis were processed without further apodization in either dimension. Peak fitting was performed in NMRPipe. Relaxation rates were determined by fitting the parameters of a monoexponential decay to experimental data using in-house Python scripts.

Theory and Results

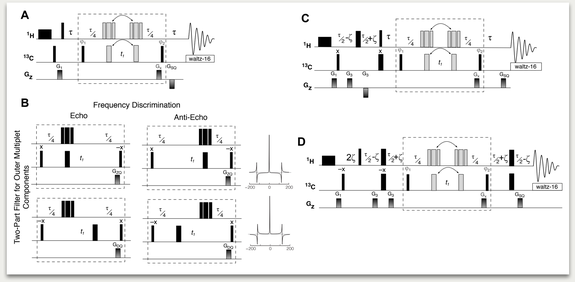

Figure 1. Gradient selected pulse sequences for measuring $^1H–^{13}C$ heteronuclear zero-quantum coherences (gsHZQC). **(A)** The basic version of the gsHZQC pulse sequence has four parts: two for inversion of the outer multiplet components and two for sensitivity-enhanced frequency discrimination during t_1, see (B) for further details. These alterations are achieved by a pulse sequence element in which the positions of the composite ^1H ($90_x–180_y–90_x$) and 180° ^{13}C pulses flanking t_1 (gray bars) are alternated. The phase of the second 90° ^{13}C pulse is inverted with the receiver during consecutive scans to form an isotope filter. All other pulse phases are {x}. G_1=(1 ms, 7 G/cm), G_{SQ} = (500 μs, 22.5 G/cm), and τ = $1/(2J_{CH})$ ≈ 3.91 ms. **(B)** The four parts of the gsHZQC can be visualized as a grid in which rows denote inversion of the outer multiple components and columns separate *N*- and *P*-type data. G_{ZQ}=(500 μs, 30 G/cm) and G_{DQ} = (500 μs, 18 G/cm). **(C** and **D)** gsHZQC pulse sequences with signal enhancement by using ^{13}C polarization. G_3 = (500 μs, 5 G/cm) and 2ζ = 1.5 ms.

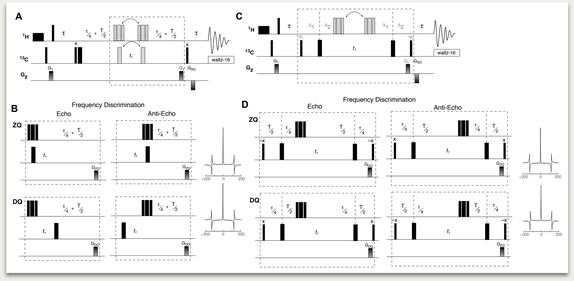

Figure 2. Hahn Echo gsHZQC pulse sequences for measurement of multiple-quantum transverse relaxation rates. **(A)** In the first part, ZQ or DQ coherence is selected during the relaxation period (T) using a pulse sequence element (see part B) similar to Figure 1B. Gradient strengths and phase cycles are as described in Figure 1A. The relaxation delay (T) is equal to $n \times 1/(2J_{CH})$ where n is any integer ≥ 1. **(B)** A grid similar to that in Figure 1B can be used to consider the precession of magnetization through the pulse sequence. In this case, the rows correspond to the multiple quantum coherence (ZQ or DQ) present during the relaxation delay and only one phase of the outer multiplet components is considered. The selection of ZQ (DQ) coherence during the relaxation delay is controlled by alternating the position of the ^{13}C 180° before (after) t_1. Frequency discrimination is again controlled by the position of composite ^1H ($90_x–180_y–90_x$) pulse. **(C)** In the second part of the relaxation experiment, the phase of the outer multiplet components is inverted relative to the first part. **(D)** The outer multiplet inversion is achieved by shifting the two ^{13}C 180° pulses between the relaxation delay (T/2) and the multiplet filtration delay (τ/4).

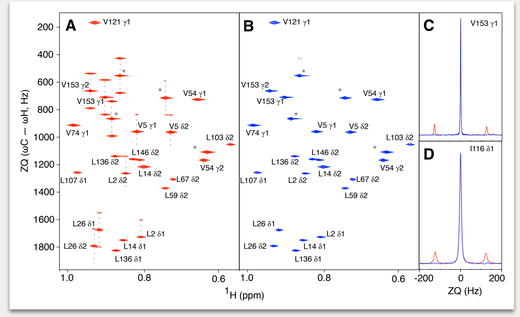

Figure 3. Comparison of the gsHZQC pulse sequence to the existing HZQC. **(A)** The ^{13}C-enhanced HZQC published by Kay and coworkers [5] of selected peaks in the methyl region of RNase H. Dashed lines connect the outer multiplet components to the central component. Unassigned peaks are marked with an asterisk. **(B)** A ^{13}C-enhanced gsHZQC (Figure 1C) of the same region. The contour levels in each data set have been normalized to their respective noise floors. **(C** and **D)** Comparison of the t_1 dimension of HZQC pulse sequences for V153 δ1 (C) and I116 δ1 (D). Colors are as in (A) and (B).

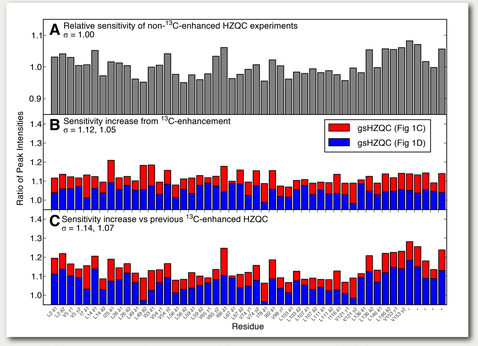

Figure 4. (A) Sensitivity of the non-^{13}C-enhanced gsHZQC sequence relative to the analogous HZQC by Kay and coworkers [4]. The gsHZQC is ~15% more sensitive than the HMQC experiment [8, 9] after normalizing for sensitivity-enhancement. **(B)** Sensitivity enhancement from ^{13}C polarization transfer. Normalized peak intensities of the ^{13}C-enhanced gsHZQC pulse sequences in Figure 1C (red) and 1D (blue) are plotted relative to the gsHZQC sequence in Figure 1A. **(C)** Sensitivity of the ^{13}C-enhanced gsHZQC experiments relative to the previous ^{13}C-enhanced HZQC pulse sequence [5]. The sensitivity improvement for the ^{13}C-enhanced gsHZQC sequences is likely due to a reduction in the number of ^1H inversion pulses.

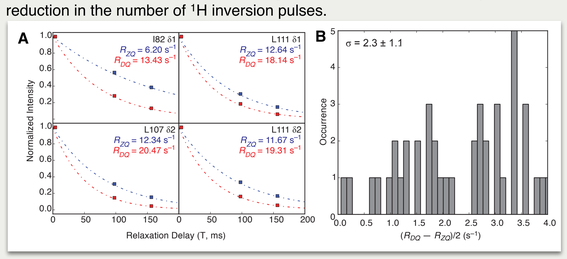

Figure 5. Measurement of multiple-quantum transverse relaxation rates in RNase H. **(A)** Zero- and double-quantum relaxation profiles, R_{ZQ} (blue) and R_{DQ} (red), for selected residues. Relaxation delays (T) were set to $n/(2J_{CH})$ were n = {1, 25, 40}. Dashed lines are the result of fitting a monoexponential decay to the respective profiles. Peak intensities were normalized for display. **(B)** Histogram of (R_{DQ} — R_{ZQ})/2 for RNase H.

Conclusions

- A gradient-selected experiment has been developed for measuring $^1H—^{13}C$ heteronuclear zero-quantum correlations in protonated methyl groups
- The resolution of the gsHZQC is improved for small proteins or large ones with flexible regions due to the active removal of outer multiple components
- Sensitivity also is improved by exciting ^{13}C magnetization in addition to ^1H magnetization
- Hahn echo variations of the gsHZQC experiment have been developed for measuring multiple-quantum transverse relaxation rates that maintain zero-quantum coherence during t_1
- The magnitude of (R_{DQ} — R_{ZQ})/2 is consistent with previous studies indicating RNase H does not undergo significant conformational exchange at these conditions [14]

Acknowledgements

A.G.P. and M.L.G. acknowledge support from National Institute of Health grants GM50291 and GM089047, respectively.

A.G.P. is a member of the New York Structural Biology Center (NYSBC). The NYSBC is a STAR center supported by the New York State Office of Science, Technology and Academic Research.

Data acquired at 18.8 and 21.1 T were collected at the NYSBC. The 900 MHz (21.1 T) spectrometers were purchased with funds from the National Institute of Health (USA), the Keck Foundation (New York State), and the NYC Economic Development Corporation.

A.G.P. and M.L.G. thank Mark Rance (University of Cincinnati) for helpful scientific discussions.

References

1. Tugarinov V. & Kay L.E. (2003) *J Am Chem Soc* **125**, 13868-78.
2. Ollerenshaw J.E., Tugarinov V. & Kay L.E. (2003) *Magn Reson Chem* **41**, 843-52.
3. Korzhnev D.M., Kloiber K., Kanelis V., Tugarinov V. & Kay L.E. (2004) *J Am Chem Soc* **126**, 3964-73.
4. Tugarinov V., Hwang P.M. & Kay L.E. (2004) *Annu Rev Biochem* **73**, 107-46.
5. Ollerenshaw J.E., Tugarinov V., Skrynnikov N.R. & Kay L.E. (2005) *J Biomol NMR* **33**, 25-41.
6. Goto N.K., Gardner K.H., Mueller G.A., Willis R.C. & Kay L.E. (1999) *J Biomol NMR* **13**, 369-74.
7. Gardner K.H. & Kay L.E. (1997) *J Am Chem Soc* **119**, 7599-600.
8. Mueller L. (1979) *J Am Chem Soc* **101**, 4481-4.
9. Bax A., Griffey R.H. & Hawkins B.L. (1983) *J Magn Reson* **55**, 301-15.
10. States D.J., Haberkorn R.A. & Ruben D.J. (1982) *J Magn Reson* **48**, 286-92.
11. Marion D. & Wuthrich K. (1983) *Biochem Biophys Res Commun* **113**, 967-74.
12. Palmer A.G., Rance M. & Wright P.E. (1991) *J Am Chem Soc* **113**, 4371-80.
13. Delaglio F., Grzesiek S., Vuister G.W., Zhu G., Pfeifer J. & Bax A. (1995) *J Biomol NMR* **6**, 277-93.
14. Mandel A., Akke M., Palmer A.G. (1995) *J Mol Bio* **246**, 144-63.